

MIRACL: A Diverse Meta-Reinforcement Learning for Multi-Objective Multi-Echelon Combinatorial Supply Chain Optimisation

Rifny Rachman*
The University of Manchester, United Kingdom

Josh Tingey
Peak AI, Ltd, United Kingdom
josh.tingey@peak.ai

Richard Allmendinger
The University of Manchester, United Kingdom
richard.allmendinger@manchester.ac.uk

Pradyumn Shukla
The University of Manchester, United Kingdom
pradyumn.shukla@manchester.ac.uk

Wei Pan
The University of Manchester, United Kingdom
wei.pan@manchester.ac.uk

Bahrul Ilmi Nasution
The University of Manchester, United Kingdom
bahrul.nasution@manchester.ac.uk

Abstract

Multi-objective reinforcement learning (MORL) is effective for multi-echelon combinatorial supply chain optimisation, where tasks involve high dimensionality, uncertainty, and competing objectives. However, its deployment in dynamic environments is hindered by the need for task-specific retraining and substantial computational cost. We introduce **MIRACL** (Meta multi-objective Reinforcement leARning with Composite Learning), a hierarchical Meta-MORL framework that allows for a few-shot generalisation across diverse tasks. MIRACL decomposes each task into structured subproblems for efficient policy adaptation and meta-learns a global policy across tasks using a Pareto-based adaptation strategy to encourage diversity in meta-training and fine-tuning. To our knowledge, this is the first integration of Meta-MORL with such mechanisms in combinatorial optimisation. Although validated in the supply chain domain, MIRACL is theoretically domain-agnostic and applicable to broader dynamic multi-objective decision-making problems. Empirical evaluations show that MIRACL outperforms conventional MORL baselines in simple to moderate tasks, achieving up to 10% higher hypervolume and 5% better expected utility. These results underscore the potential of MIRACL for robust, efficient adaptation in multi-objective problems.

Keywords: Multi-objective optimisation, Reinforcement Learning, Meta-learning, Combinatorial problems, Supply chain.

*Corresponding author. Email: rifny.rachman@manchester.ac.uk

1 Introduction

Multi-echelon combinatorial supply chain (SC) optimisation is challenging due to the scale and interdependence of facilities, echelons, and transportation routes, further compounded by conflicting objectives, uncertainty, and parameter fluctuations. Multi-objective reinforcement learning (MORL), formulated as a multi-objective Markov decision process (MOMDP), has been developed to address such settings by learning sequential decisions through continuous agent–environment interaction (Shar et al., 2023; Zhao and Lou, 2025; Rachman et al., 2025; Sutton and Barto, 2015). MORL can adapt to feedback, respond to operational changes, and recover trade-off solutions, but often requires substantial computation due to exploration-intensive trial-and-error.

In practice, MORL policies are typically specialised to a given SC configuration, so changes in architecture or parameters require retraining. This is problematic in dynamic operations where costs, lead times, and network connectivity can shift (e.g., route disruptions) and decisions must be made quickly. Meta-learning for MORL (Meta-MORL) aims to reduce this burden by *learning how to learn* across tasks with different configurations, enabling rapid adaptation to new instances without repeating full training (Schmidhuber, 1987; Finn et al., 2017; Thrun and Pratt, 1998).

However, Meta-MORL remains underexplored in SC: existing work focuses mainly on inventory control (Wang et al., 2024) and combinatorial vehicle routing (Zhang et al., 2023). Moreover, prior combinatorial approaches often meta-train over decomposed subproblems within a single problem type, which limits generalisation when both decision variables and parameters vary substantially. These limitations are particularly salient in multi-echelon SC problems, where task heterogeneity is larger, and meta-training can be unstable.

To address this gap, we cast multi-objective, multi-echelon combinatorial SC optimisation as a MOMDP meta-learning problem and propose **MIRACL** (**M**eta **m**ult**I**-objective **R**einforcement **l**e**A**rning with **C**omposite **L**earning). MIRACL extends Meta-MORL by (i) using hierarchical composite learning to organise adaptation through multiple within-task scalarised subproblems, and (ii) introducing an archive-guided Pareto simulated annealing (PSA) mechanism that perturbs preference weights during meta-training to promote broader PF coverage beyond passive sampling. MIRACL further applies the same PSA-based weight adaptation during fine-tuning, where the weight updates more directly translate into diverse final solutions on the target task. We evaluate MIRACL against conventional MORL methods and a metaheuristic on SC instances of increasing complexity, and analyse the resulting operational behaviours to highlight when each approach is most effective and the trade-offs they induce in practice. Moreover, we demonstrate MIRACL’s domain-agnosticism beyond SC.

2 Related Work

Recent MORL advances aim to learn *preference-aware* policies while improving PF coverage. Most remain utility-based, using scalarisation to make trade-offs explicit: envelope Q-learning generalises across linear preferences (Yang et al., 2019), and Pareto-conditioned networks capture mul-

multiple trade-offs via preference conditioning (Reymond et al., 2022). For high-dimensional control, MORL based on decomposition (MORL/D) decomposes learning into scalarised subproblems with continuous policies (Felten et al., 2023b), fitting multi-echelon SC where decisions scale, and preferences shift. Yet MORL alone is sample-intensive and often requires retraining as tasks change, motivating meta-RL for rapid adaptation (e.g., RL² and MAML) (Duan et al., 2016; Finn et al., 2017).

Meta-MORL (Chen et al., 2019) bridges this gap by targeting generalisation across both tasks and preferences. Liu and Qian (2021) extend Meta-MORL with a predictor that selects weights to maximise expected PF improvement in continuous control, but they meta-train on a single task decomposed by weight vectors rather than across distinct tasks. Lu et al. (2024) detect environment changes via an unsupervised auto-encoder and treat them as contexts for a Reptile-based meta-learner (Nichol et al., 2018) with generalised policy improvement. Al-Habob et al. (2024) apply Meta-MORL to vehicular networks by decomposing into subproblems, training per-subproblem, and using MAML to learn a transferable initialisation.

Although the application of Meta-MORL in the SC domain appears to have great potential, there is a scarcity of research concentrating on this area. For example, Wang et al. (2024) applied MAML along with proximal policy optimisation (PPO) to address a single-facility inventory issue, while Zhang et al. (2023) utilised Reptile with actor-critic reinforcement learning (RL) to solve travelling salesman and vehicle routing problems. Consequently, the opportunities for exploration in this domain remain substantial, particularly in complex multi-echelon structures like SC network design.

3 Problem Definition

We formulate the combinatorial SC optimisation problem as a finite-horizon MOMDP (Hayes et al., 2022), where each episode represents a sequence of operational decisions over time t within time horizon T . The tuple $\langle \mathcal{S}, \mathcal{A}, ST, \gamma, \mu, \mathbf{R} \rangle$, where: \mathcal{S} is the state space, including inventory levels, outstanding orders, cumulative emissions, and average service level (SL) inequality; \mathcal{A} is the action space, including manufacturing and delivery quantities; $ST : \mathcal{S} \times \mathcal{A} \rightarrow \mathcal{S}$ is the state transition function that governs how states evolve given actions; $\gamma \in [0, 1]$ is the discount factor; μ is the initial state distribution; and $\mathbf{R} : \mathcal{S} \times \mathcal{A} \rightarrow \mathbb{R}^d$ is a vector-valued reward function that captures conflicting objectives d , such as profit, emissions, and SL inequality. We denote the instantaneous vector reward on subproblem k by $\mathbf{r}_k(\mathbf{s}_t, \mathbf{a}_t) = \mathbf{R}_k(\mathbf{s}_t, \mathbf{a}_t)$, where \mathbf{s}_t and \mathbf{a}_t represent the state and action at period t , respectively. The agent’s goal is to learn a policy $\pi_\theta(\mathbf{a} \mid \mathbf{s})$ that approximates the PF over the expected cumulative rewards. The SC-specific MOMDP formulation simulated in this paper is based on the previous study (Rachman et al., 2026), provided in Appendix B.

To enable generalisation across a distribution of SC tasks, we adopt a gradient-based meta-learning using RL framework that learns an initial policy parameterisation θ capable of rapid adaptation. Each task \mathcal{T} is sampled from a task distribution $p(\mathcal{T})$, defined as a finite-horizon

MOMDP with transition dynamics $ST_{\mathcal{T}}$, initial state distribution $\mu_{\mathcal{T}}$, and reward function $\mathbf{R}_{\mathcal{T}}$. Following Finn et al. (2017), each task is associated with a loss function:

$$\mathcal{L}_{\mathcal{T}_k}(\pi_{\theta'_k}) = -\mathbb{E}_{\mathbf{s}_t, \mathbf{a}_t \sim \pi_{\theta'_k}, \mu_{\mathcal{T}_k}} \left[\sum_{t=1}^T \mathbf{w}_k^\top \mathbf{r}_k(\mathbf{s}_t, \mathbf{a}_t) \right], \quad (1)$$

where $\mathbf{w}_k \in \mathbb{R}^d$ is a task-specific weight vector used to scalarise multiple objectives.

During the adaptation phase, the meta-policy π_{θ} is fine-tuned to each sampled task \mathcal{T}_k via gradient descent for α adaptation step size, yielding adapted parameters θ'_k , where:

$$\theta'_k = \theta - \alpha \nabla_{\theta} \mathcal{L}_{\mathcal{T}_k}(\pi_{\theta}). \quad (2)$$

In the meta-update phase, the meta-parameters θ are updated by aggregating losses across tasks drawn from the distribution $p(\mathcal{T})$, as follows:

$$\theta = \arg \min_{\theta} \sum_{\mathcal{T}_k \sim p(\mathcal{T})} \mathcal{L}_{\mathcal{T}_k}(\pi_{\theta'_k}). \quad (3)$$

This two-stage process enables the agent to quickly adapt to new SC tasks using limited interaction.

4 Methods

This section presents the mechanism of the arrangement of the SC tasks, the algorithm we use in this study, and the performance measurement.

4.1 Meta-MORL Algorithm

Chen et al. (2019) extends MAML to multi-objective RL by learning a meta-policy that rapidly adapts to different scalarisation preferences. Training has three stages: (i) *adaptation*, scalarising each sampled task with a weight vector and performing a few inner updates; (ii) *meta-learning*, updating meta-parameters across scalarised tasks to learn a transferable initialisation; and (iii) *fine-tuning*, applying multiple weights on an unseen task to train candidate policies that are non-dominated sorted to approximate the PF. Although this supports generalisation across tasks and preferences, Meta-MORL samples tasks and weights independently each iteration, which can increase update variance when successive batches differ in dynamics or preferences. In high-dimensional combinatorial SC problems, this variability can weaken limited-step adaptation, motivating more structured within-task training and explicit diversity mechanisms.

4.2 Proposed Algorithm

We introduce MIRACL, an algorithm to promote solution diversity of current Meta-MORL by optimising through nested scalarised tasks. This method minimises variability across trained tasks

in the adaptation phase by processing a set of similar subproblems with varied weights before transitioning to a different task. In addition, it incorporates a mechanism to explicitly improve task diversity for better learning in a more exploited search area. MIRACL builds upon MAML and Meta-MORL, both of which are established as general-purpose meta-learning frameworks applicable across diverse domains. Its hierarchical learning and PSA-based adaptation operate purely on objective structures, not domain-specific assumptions.

4.2.1 Hierarchical composite learning

As in Meta-MORL, we assume a task distribution $p(\mathcal{T})$, a weight distribution $p(\mathbf{w})$, and step sizes α and β for inner adaptation and meta-updates. MIRACL introduces *hierarchical composite learning*: for each sampled task, we decompose the same SC instance into K scalarised subproblems by applying different weight vectors on the simplex (Figure 1). We use linear scalarisation by default, but MIRACL is agnostic to the scalarisation form and can be combined with alternatives (e.g., Tchebycheff (Van Moffaert et al., 2013)). Unlike Meta-MORL, which treats sampled weights as fixed, MIRACL updates the K weights after each meta-update using an *archive-guided PSA* rule, steering subproblems toward under-covered regions of objective space without additional rollouts.

Processing multiple subproblems under the same task dynamics provides a more stable adaptation signal and enables the diversity mechanism. We initialise the meta-policy π_θ and maintain an archive of non-dominated vector returns across tasks and subproblems to guide PSA throughout meta-training. Standard Meta-MORL samples independent pairs $(\mathcal{T}, \mathbf{w})$, entangling task and preference variation within a batch. MIRACL instead conditions on a task \mathcal{T} and evaluates $\{\mathbf{w}_k\}_{k=1}^K$ under shared dynamics, while PSA perturbs weights using the archive to discourage revisiting previously explored objective regions and to improve coverage.

Variance reduction intuition. Let $G(\mathcal{T}, \mathbf{w})$ denote the meta-gradient contribution obtained after inner adaptation under task \mathcal{T} and preference weight \mathbf{w} : $G(\mathcal{T}, \mathbf{w}) := \nabla_\theta \mathcal{L}_\mathcal{T}(\pi_{\theta'})$, where θ' is produced by Equation (2) and $\mathcal{L}_\mathcal{T}$ is the scalarised loss using weight \mathbf{w} (as in Equation (1)). We denote the meta-gradient estimator at a given iteration as $\hat{G}_{\text{Meta}} = \frac{1}{B} \sum_{i=1}^B G(\mathcal{T}_i, \mathbf{w}_i)$ for Meta-MORL, and $\hat{G}_{\text{MIRACL}} = \frac{1}{K} \sum_{k=1}^K G(\mathcal{T}, \mathbf{w}_k)$ for MIRACL (where MIRACL uses a single task \mathcal{T} with K weights). By the law of total variance (Casella and Berger, 2002), Meta-MORL satisfies:

$$\text{Var}(\hat{G}_{\text{Meta}}) = \underbrace{\mathbb{E}_{\{\mathcal{T}_i\}} \left[\text{Var} \left(\frac{1}{B} \sum_{i=1}^B G(\mathcal{T}_i, \mathbf{w}_i) \mid \{\mathcal{T}_i\} \right) \right]}_{\text{preference-induced variance across heterogeneous tasks}} + \underbrace{\text{Var}_{\{\mathcal{T}_i\}} \left(\mathbb{E}_{\{\mathbf{w}_i\}} \left[\frac{1}{B} \sum_{i=1}^B G(\mathcal{T}_i, \mathbf{w}_i) \mid \{\mathcal{T}_i\} \right] \right)}_{\text{task-induced variance}}, \quad (4)$$

where $\{\mathcal{T}_i\}_{i=1}^B$ is a batch of B tasks sampled at a given meta-iteration. Conditioning on $\{\mathcal{T}_i\}$ isolates the variance due to weight sampling for this fixed task set.

In contrast, MIRACL conditions on a *single* task \mathcal{T} within the meta-iteration. Since all K subproblems share the same transition dynamics $ST_\mathcal{T}$, their gradient contributions $\{G(\mathcal{T}, \mathbf{w}_k)\}_{k=1}^K$

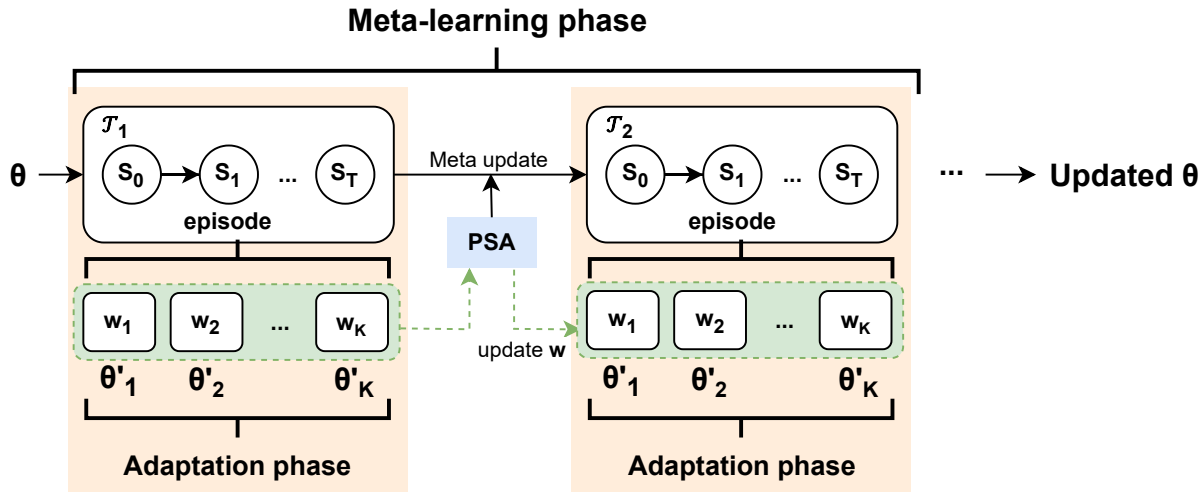


Figure 1: Meta-learning and adaptation phases in MIRACL. Each task is decomposed using several weight vectors, then PSA is applied between meta-updates to improve the task diversity.

are correlated through the task structure. The within-iteration (preference-induced) variance thus admits the covariance expansion:

$$\text{Var}(\hat{G}_{\text{MIRACL}} | \mathcal{T}) = \frac{1}{K^2} \sum_{k=1}^K \text{Var}(G(\mathcal{T}, \mathbf{w}_k) | \mathcal{T}) + \frac{2}{K^2} \sum_{1 \leq k < \ell \leq K} \text{Cov}(G(\mathcal{T}, \mathbf{w}_k), G(\mathcal{T}, \mathbf{w}_\ell) | \mathcal{T}). \quad (5)$$

Taking expectation over $\mathcal{T} \sim p(\mathcal{T})$ yields:

$$\text{Var}(\hat{G}_{\text{MIRACL}}) = \mathbb{E}_{\mathcal{T}} \left[\text{Var}(\hat{G}_{\text{MIRACL}} | \mathcal{T}) \right] + \text{Var}_{\mathcal{T}} \left(\mathbb{E}_{\{\mathbf{w}_k\}} \left[\hat{G}_{\text{MIRACL}} | \mathcal{T} \right] \right). \quad (6)$$

Meta-MORL aggregates gradients from different tasks and preferences within a meta-batch, whereas MIRACL first averages K preference-conditioned gradients under fixed task dynamics. In Equation (5), the $1/K^2$ factors come from this averaging, and the covariance term reflects cross-preference gradient alignment. When gradients are not nearly identical (i.e., not perfectly aligned), the covariance is not dominant, so within-task averaging behaves like a sample mean: preference-driven variance shrinks as $1/K$ (standard deviation $1/\sqrt{K}$). Hence, MIRACL reduces preference-induced fluctuations in each task’s meta-update. This discussion aims to build intuition rather than provide a direct measurement. Empirically tracking meta-gradient variance would require checkpoint-level logging throughout meta-training, which we do not have for the runs reported. We therefore use observed experimental trends as indirect evidence and leave a thorough empirical verification to future work.

Algorithm 1 instantiates this process: line 3 samples a single task \mathcal{T} , lines 9–14 compute K adapted gradients under shared dynamics (yielding the covariance structure in Equation (5)), line 15

applies the meta-update using $\widehat{G}_{\text{MIRACL}}$, and the diversity mechanism applies PSA to update weights using the archive. The meta-learner operates over tasks $\mathcal{T} \sim p(\mathcal{T})$ through an N -shot trajectory $D = \{(\mathbf{s}_1, \mathbf{a}_1, \dots, \mathbf{s}_T)\}$: each \mathcal{D}_k is collected by executing π_θ on \mathcal{T}_k , inner-loop adaptation yields task-specific θ'_k , and the outer loop updates θ using $\mathcal{L}_{\mathcal{T}_k}$.

Algorithm 1 Meta-training Phase of MIRACL

Require: Task distribution $p(\mathcal{T})$, weight distribution $p(\mathbf{w})$, number of subproblems K , step sizes α, β

- 1: **Initialise:** meta-policy π_θ , archive $\leftarrow \emptyset$
- 2: **while** not done **do**
- 3: Sample a task $\mathcal{T} \sim p(\mathcal{T})$
- 4: **if** archive = \emptyset **then**
- 5: Generate K normalised weights $\{\mathbf{w}_1, \dots, \mathbf{w}_K\} \sim p(\mathbf{w})$
- 6: **else**
- 7: Generate K weights $\{\mathbf{w}_1, \dots, \mathbf{w}_K\}$ from archive
- 8: **end if**
- 9: **for** $k = 1$ to K **do**
- 10: Form subproblems \mathcal{T}_k using $(\mathcal{T}, \mathbf{w}_k)$
- 11: Rollout \mathcal{D}_k using π_θ in \mathcal{T}_k
- 12: Compute $\theta'_k \leftarrow \theta - \alpha \nabla_{\theta} \mathcal{L}_{\mathcal{T}_k}(\pi_\theta)$
- 13: Evaluate reward \mathbf{r}_k in \mathcal{T}_k using $\pi_{\theta'_k}$
- 14: **end for**
- 15: Meta-update $\theta \leftarrow \theta - \beta \nabla_{\theta} \sum_k \mathcal{L}_{\mathcal{T}_k}(\pi_{\theta'_k})$
- 16: Update \mathbf{w} via DiversityMechanism($\mathcal{T}, \mathbf{w}, \mathbf{r}$, archive)
- 17: **end while**
- 18: **return** Updated meta-policy π_θ

4.2.2 Diversity mechanism

In Meta-MORL, each task is scalarised by sampling a preference vector $\mathbf{w} \sim p(\mathbf{w})$ and adapting from a shared meta-policy π_θ . While this enables efficient multi-objective learning and cross-task generalisation, it also couples early exploration across subproblems: within a meta-batch, trajectories are generated from the same initial policy before inner-loop adaptation. As a result, the diversity of collected experience is largely determined by the coverage of $p(\mathbf{w})$ and by the capacity of the adaptation step to separate behaviours across weights. When $p(\mathbf{w})$ under-explores the simplex or adaptation is shallow, the meta-policy may concentrate on a narrow subset of trade-offs and generalise poorly to unseen preferences.

We address this limitation by introducing a *diversity mechanism* that actively perturbs the K subproblem weights after each meta-update. Specifically, we employ Pareto Simulated Annealing (PSA) (Czyżżak and Jaskiewicz, 1998) to update $\{\mathbf{w}_k\}_{k=1}^K$ using the archive of previously evaluated objective vectors. After normalising objectives to $[0, 1]$, we find for each \mathbf{r}_k its nearest archived neighbour \mathbf{r}'_k (Euclidean distance) and adjust each weight component w_k^j according to the PSA rule in Equation (7). Intuitively, the archive acts as a reference set, and PSA encourages successive

subproblems to move away from existing solutions, promoting broader coverage of the PF set.

$$w_k^j = \begin{cases} w_k^j \times (1 + \delta), & \text{if } r_k^j \geq r_k'^j, \\ w_k^j / (1 + \delta), & \text{if } r_k^j < r_k'^j. \end{cases} \quad (7)$$

The update is applied component-wise for $j = 1, \dots, d$ (with d objectives). For minimisation objectives (e.g., emissions, inequality), we sign-flip rewards so that larger values always indicate better performance before comparison.

Algorithm 2 Diversity Mechanism (with PSA)

Require: Task \mathcal{T} , weights $\{\mathbf{w}_1, \dots, \mathbf{w}_K\}$, rewards $\{\mathbf{r}_1, \dots, \mathbf{r}_K\}$, archive, PSA steps S , PSA rate δ

```

1: for  $s = 1$  to  $S$  do
2:   for  $k = 1$  to  $K$  do
3:     if archive  $\neq \emptyset$  then
4:       Find closest reward  $\mathbf{r}'$  in archive to  $\mathbf{r}_k$ 
5:       Update  $\mathbf{w}_k$  using PSA rule (Equation (7))
6:       Normalise  $\mathbf{w}_k \leftarrow \mathbf{w}_k / \|\mathbf{w}_k\|_1$ , with  $\mathbf{w}_k \geq 0$ 
7:     end if
8:   end for
9: end for
10: for  $k = 1$  to  $K$  do
11:   if  $\mathbf{r}_k$  is non-dominated w.r.t. archive then
12:     Add  $\mathbf{r}_k$  to archive
13:   end if
14: end for
15: return Updated  $\mathbf{w}$ , archive

```

Algorithm 2 applies PSA after task decomposition: given \mathcal{T} , $\{\mathbf{w}_k\}_{k=1}^K$, $\{\mathbf{r}_k\}_{k=1}^K$, and the archive (with fixed S and δ), it updates each \mathbf{w}_k using its nearest archived neighbour, then renormalises onto the simplex. Finally, newly obtained non-dominated \mathbf{r}_k are added to the archive.

4.2.3 Fine-tuning phase

After meta-learning, the trained meta-policy initialises fine-tuning, where the agent adapts to an unseen task in a few gradient steps. To approximate the PF, we train a set of scalarised policies using randomly sampled weights over the preference simplex, which avoids concentrating training on a small set of fixed trade-offs and remains practical as the number of objectives grows. Each sampled weight defines one scalarised subproblem, and we train each corresponding solution separately with the chosen RL algorithm, for example, PPO.

The PSA-based weight diversity mechanism is applied only at the end of fine-tuning rather than throughout training. This approach aligns with meta-learning principles. Since all policies start from the same meta-policy, early PSA application would be ineffective when policies remain similar. Delaying PSA until after fine-tuning allows policies to first specialise toward their assigned

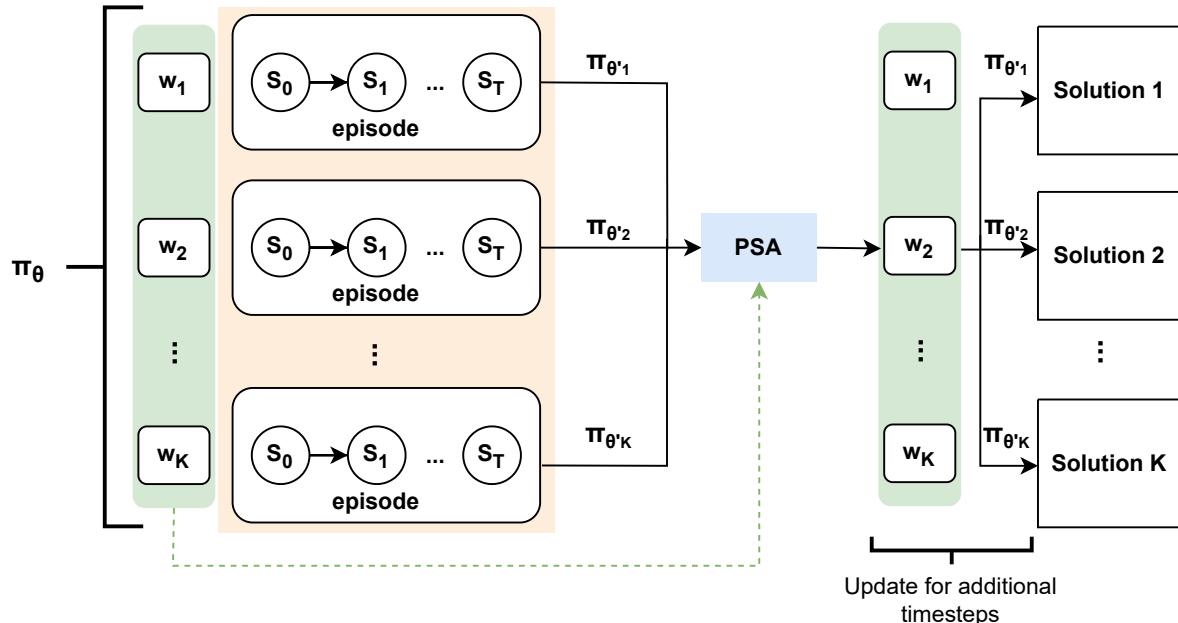


Figure 2: Fine-tuning phase requires only a few shots training since it utilises the meta-policy as a good initialisation.

weights before targeted refinement, making diversity enhancement more effective. The detailed pseudocode is provided in Appendix C.

5 Experiments

This section outlines the settings for the meta-training and fine-tuning phases in our experiments. We conducted our experiments using Python 3.11.2 on JupyterLab with 128 GB RAM and a 16-core CPU. We train the algorithms on three complexities of the SC environment shown in Table 1. Each instantiation is repeated ten times for statistical robustness. SC networks are configured as collections of nodes that are interconnected by edges. Additional SC configuration and environment details are in Appendix D.

Table 1: SC environments simulated in our experiment. Each environment complexity corresponds with the action and observation space dimension, number of nodes, and edges.

Complexities	Action	Observation	Nodes	Edges
Simple	8	20	7	8
Moderate	21	49	13	21
Complex	59	131	24	59

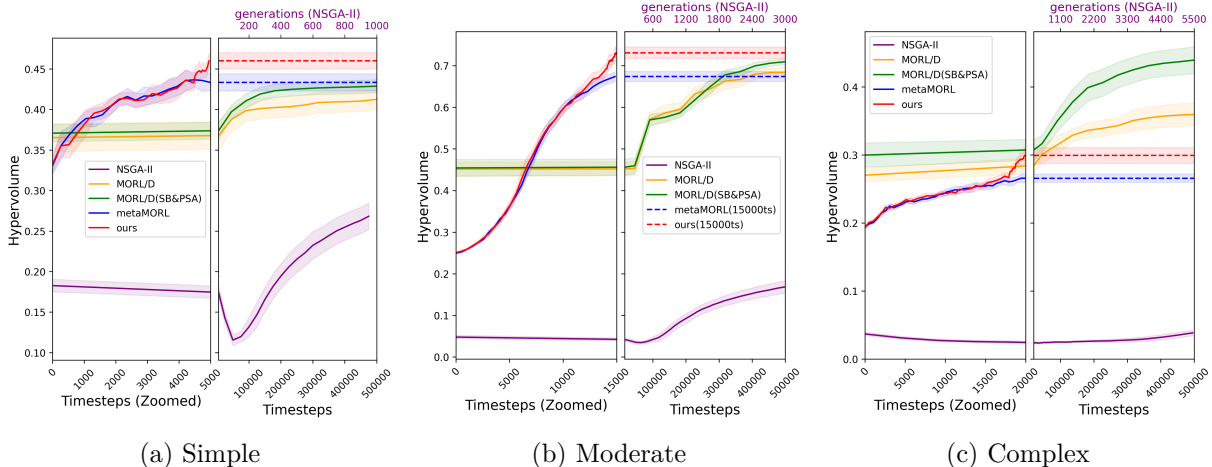


Figure 3: Normalised hypervolume comparison of MORL/D, MORL/D with SB and PSA, NSGA-II, Meta-MORL, and our proposed methods. Left panels show early time steps (proportional to NSGA-II generations), while right panels show later iterations. MIRACL consistently outperforms all baseline methods in simple (3a) and moderate problems (3b), but is exceeded by MORL/D in complex ones (3c).

Table 2: Runtime comparison (in minutes) between MIRACL and traditional algorithms. Meta-training time (MT) is reported separately as a one-off overhead (using 4 parallel workers), while fine-tuning time (FT) reflects the per-task cost.

Algorithms	Simple	Moderate	Complex
MIRACL(MT)	8	12	14
MIRACL(FT)	14	47	77
MORL/D	84	95	111
NSGA-II	2	10	47

5.1 Algorithm Settings

We report meta-training and fine-tuning settings for MIRACL and baselines, with detailed hyperparameters provided in Appendix E. Minimisation objectives (emissions and inequality) are sign-flipped, and all objectives are normalised to $[0, 1]$ prior to scalarisation and nearest-neighbour comparisons.

5.2 Meta-training settings

We implement MAML (Finn et al., 2017) with PPO (Schulman et al., 2017) in Ray RLlib 2.3.1 (Liang et al., 2017), extended to support Meta-MORL and MIRACL. Meta-training runs for 10^6 environment steps on randomly generated SC tasks. In each meta-iteration, a task is sampled and decomposed into subproblems. Then, inner-loop adaptation is performed, and a meta-update is applied to the shared policy. We use four inner adaptation steps for simple problems and eight for moderate and complex cases, balancing fast adaptation and task-specific learning. A meta-environment

Table 3: Performance comparison between Meta-MORL and MIRACL. MIRACL is evaluated with PSA applied only in meta-training (MT) or in both meta-training and fine-tuning (MT&FT). We report hypervolume, sparsity, and EUM, with Δ indicating the percentage change relative to Meta-MORL. Statistical significance is assessed via a Kruskal–Wallis test followed by Dunn’s post hoc tests with Bonferroni correction, where *, **, and *** denote $p < 0.05$, $p < 0.01$, and $p < 0.001$, respectively.

Problems	Aspects	Meta-MORL	MT	MT&FT	Δ MT	Δ MT&FT
Simple	Hypervolume	0.4333	0.4460	0.4600	2.92%	6.16%**
	Sparsity	0.0056	0.0052	0.0057	-8.03%	1.36%
	EUM	0.7075	0.7398	0.7436	4.57%	5.10%**
Moderate	Hypervolume	0.6737	0.6853	0.7306	1.73%	8.45%***
	Sparsity	0.0015	0.0025	0.0013	71.75%*	-7.78%
	EUM	0.8387	0.8538	0.8394	2.75%*	1.03%
Complex	Hypervolume	0.2658	0.2668	0.2993	0.38%	12.62%***
	Sparsity	0.0022	0.0016	0.0032	-25.77%	44.78%*
	EUM	0.6118	0.6176	0.6236	-0.35%	1.79%

wrapper enables dynamic task sampling to reflect realistic task variation.

To promote diversity, MIRACL applies 10 PSA steps after each meta-update. We sample weights \mathbf{w} uniformly from the 3D simplex using Dirichlet(1,1,1) and solve $K = 10$ scalarised subproblems per meta-iteration with a fixed PSA rate $\delta = 0.05$. We use linear scalarisation for its simplicity and smooth optimisation signal when training many subproblems in high-dimensional combinatorial settings. Noting that it may under-represent non-convex PF regions, we therefore include a Linear vs. Tchebycheff ablation under the same budget and protocol. MIRACL maintains a global archive of non-dominated (normalised) reward vectors across tasks, which guides PSA weight updates. Training stability is improved via PPO clipping, Kullback–Leibler regularisation, and generalised advantage estimation.

5.3 Fine-tuning settings

Fine-tuning uses the Messiah SC simulator (Rachman et al., 2026) for 5,000, 15,000, and 20,000 steps on simple, moderate, and complex tasks, respectively, which is substantially fewer than training-from-scratch RL baselines (typically $\sim 500,000$ steps in our SC setup). The number of shots matches meta-training, and observation/action spaces are normalised.

As PPO is single-objective, we scalarise vector rewards with simplex-projected weights. For each task, we train 21 weighted agents ($K = 21$) across 10 seeds (210 runs) and obtain 10 PF approximation sets via non-dominated sorting (Rachman et al., 2025). We use generalised advantage estimation with advantage normalisation to reduce variance, and a standard multi-layer perceptron policy architecture. Experiments are conducted on three SC environments of increasing network complexity (simple, moderate, complex).

5.4 Results and Discussion

We evaluate MIRACL on multiple SC settings, comparing its fine-tuning performance with Meta-MORL and standard MORL baselines (Rachman et al., 2026): MORL/D, its shared-buffer (SB) variant that shares trajectories across policies, and the classical NSGA-II. All methods are tested on similar unseen tasks. Performance is measured by normalised hypervolume (Zitzler and Thiele, 1998) with reference point (0,0,0) after sign-flipping minimisation objectives; the expected utility metric (EUM) (Hayes et al., 2022), $EUM = \frac{1}{|\mathcal{W}|} \sum_{\mathbf{w} \in \mathcal{W}} \max_{\pi \in \Pi} \mathbf{w}^\top \mathbf{r}(\pi)$, using weight vectors \mathbf{w} uniformly sampled from the 3-dimensional simplex; and sparsity, the average squared distance between consecutive Pareto solutions used as a diversity indicator (Xu et al., 2020). Higher hypervolume and EUM indicate better performance, while lower sparsity corresponds to a denser solution set.

5.4.1 Traditional method comparison

Figure 3 shows that MIRACL achieves about 10% and 6% higher normalised hypervolume than the baselines on the simple and moderate tasks, respectively, while using substantially fewer fine-tuning time steps. In the complex task, MIRACL is roughly 20% below MORL/D but converges faster and generalises better than NSGA-II, which performs worst overall. Across 10 runs per method per setting, Kruskal–Wallis detects significant differences ($p < 0.001$). Dunn’s post hoc tests with Bonferroni correction confirm MIRACL outperforms NSGA-II in all settings ($p < 0.001$), and also MORL/D in the simple task and Meta-MORL in the moderate task ($p < 0.05$). Where differences are significant, MIRACL attains the higher hypervolume. In the complex task, the deficit to MORL/D is not statistically significant, suggesting competitiveness under increased complexity. The remaining gap likely stems from the few-shot adaptation difficulty in highly complex environments. It can be reduced through longer fine-tuning or repeated PSA to allow the solutions to spread more, covering a larger hypervolume area, at a higher computational cost.

Table 2 reports wall-clock runtimes on the resource in Section 5 (Meta-MORL omitted as its runtime is comparable to MIRACL). MIRACL incurs a one-off meta-training cost with four parallel rollout workers, then reuses the meta-policy for fast per-task fine-tuning. Despite this, it is consistently faster than MORL/D across all complexities. NSGA-II is the cheapest but degrades on harder instances, highlighting MIRACL’s favourable upfront–per-task trade-off. Meta-learning targets *per-task* sample efficiency: MIRACL is evaluated in a few-shot fine-tuning regime, whereas MORL/D and NSGA-II train from scratch.

5.4.2 Ablation studies

We conduct some ablations to validate MIRACL’s design choices and assess component contribution. Table 3 focuses on the diversity mechanism, showing that PSA is most beneficial for improving solution quality. Using PSA during meta-training (MT) yields consistent hypervolume gains across all problem complexities, consistent with broader exposure to diverse trade-offs during inner-loop adaptation and improved generalisation. Applying PSA again after fine-tuning

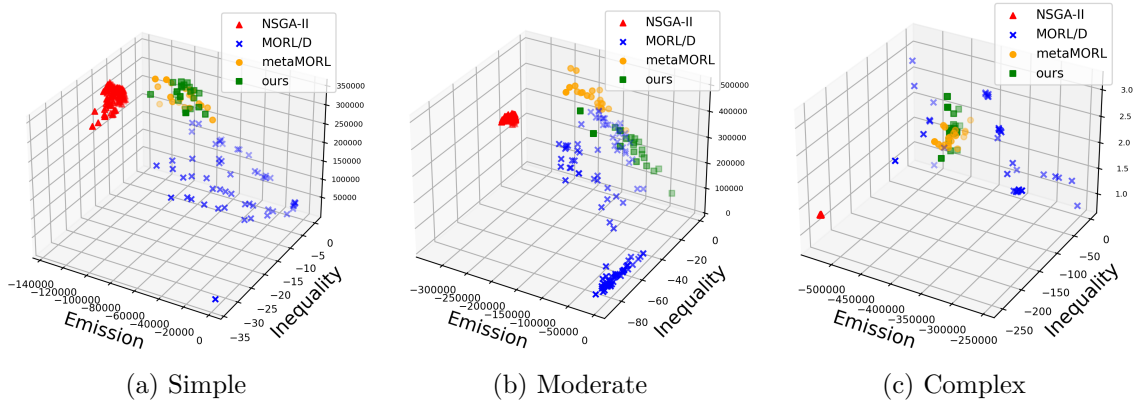


Figure 4: PF approximation sets of NSGA-II, MORL/D, Meta-MORL, and MIRACL across simple, moderate, and complex SC problems. Meta-learning-based methods produce more diverse solutions than NSGA-II, yet, more concentrated than MORL/D. The concentration increases with the problem complexity.

(MT&FT) further increases hypervolume and produces the greatest improvements, particularly as complexity grows. These hypervolume gains are statistically significant under Kruskal–Wallis with Bonferroni-corrected Dunn post hoc tests. EUM generally improves in tandem, while sparsity effects are mixed, suggesting PSA primarily prioritises non-dominated solution quality and may trade off frontier spacing depending on when it is applied. Moreover, we conduct ablation on PSA Parameters (K, S, δ) and scalarisation methods (including Tchebycheff (Van Moffaert et al., 2013)), which is presented in Appendix F.2.

5.4.3 Algorithm solutions analysis

We visualise PF approximations using best-performing runs for each algorithm, as shown in Figure 4. Meta-learning methods produce competitive solutions with moderate concentration and low sparsity, indicating stability but limited diversity. MIRACL converges to high-quality regions, achieving high profit, low emissions, and low inequality. In simpler problems, it prioritises profit at the cost of higher emissions while maintaining lower inequality than MORL/D. A strong profit–emissions trade-off emerges, while inequality shows weaker correlation with other objectives. In complex settings, meta-learning methods yield more concentrated PFs due to few-shot adaptation constraints. However, MIRACL spans a broader range of profit outcomes with moderate emissions and inequality, outperforming NSGA-II in both diversity and optimality, demonstrating the value of PSA-based diversity mechanisms for better PF exploration. We further examine the operational behaviour and found that MIRACL achieves the most consistent production and inventory profiles over time, as discussed in detail in Appendix F.4.

Table 4: Cross-domain benchmarks (mean over 10 runs). The asterisk (*) denote statistically significantly different results using the Wilcoxon test on $p < 0.05$, respectively against Meta-MORL.

Algorithm	Hypervolume	Sparsity	EUM
<i>mo-hopper-v4</i>			
MIRACL	0.1108*	0.0234*	0.4003*
Meta-MORL	0.0756	0.0047	0.3718
<i>mo-halfcheetah-v4</i>			
MIRACL	0.7002	0.0143	0.6910
Meta-MORL	0.6556	0.0114	0.6655
<i>resource-gathering-v0</i>			
MIRACL	0.7000	0.2051	0.7288
Meta-MORL	0.7000	0.1927	0.7727

5.5 Domain-Agnostic MIRACL

We evaluate MIRACL on three MO-Gymnasium benchmarks (Felten et al., 2023a): *mo-hopper-v4*, *mo-halfcheetah-v4* (continuous, unbounded rewards), and *resource-gathering-v0* (discrete, bounded rewards). As shown in Table 4, MIRACL demonstrates strong generalisation capabilities, particularly in continuous control tasks. It significantly outperforms Meta-MORL ($p < 0.05$) across all metrics in *mo-hopper-v4* and achieves higher hypervolume and EUM in *mo-halfcheetah-v4*. In the discrete *resource-gathering-v0* task, MIRACL remains competitive, matching Meta-MORL’s hypervolume with comparable EUM and sparsity. These results confirm that MIRACL’s can also extend beyond SC environments.

6 Conclusions and Future Works

Our results show that meta-learning methods, including MIRACL, perform well in simple and moderate tasks with significantly fewer training steps than traditional RL. In complex scenarios, performance remains comparable. While meta-learning yields denser and more robust solution sets, this may reduce diversity. Integration of PSA-based diversity into MIRACL fine-tuning improves hypervolume, EUM, and sparsity, especially under higher task complexity. PF approximations show that both meta-learning-based and traditional MORL solutions often share solution areas. However, meta-learning achieves more clustered sets, particularly in complex tasks, although not as severe as NSGA-II. As tasks grow more complex, it is crucial to balance rapid adaptation with adequate exploration to improve exploration in meta-learning, such as by combining different meta-policy training methods.

Acknowledgements The authors acknowledge the funding granted by the Economic and Social Research Council of UK Research and Innovation, the University of Manchester, and Peak AI, Ltd, with grant reference number ES/T002085/1. Research is carried out using computational resources

from The University of Manchester and Peak AI, Ltd. We also acknowledge that the Peak AI, Ltd. Data Science team is involved in *Messiah* development.

References

- Al-Habob, A.A., Tabassum, H., Waqar, O., 2024. Non-orthogonal age-optimal information dissemination in vehicular networks: a meta multi-objective reinforcement learning approach. *IEEE Transactions on Mobile Computing* 23, 9789–9803. doi:10.1109/TMC.2024.3367166.
- Casella, G., Berger, R.L., 2002. *Statistical Inference*. 2nd ed., Duxbury Press.
- Chen, X., Ghadirzadeh, A., Bjorkman, M., Jensfelt, P., 2019. Meta-Learning for Multi-objective Reinforcement Learning, in: 2019 IEEE/RSJ International Conference on Intelligent Robots and Systems (IROS), IEEE, Macau, China. pp. 977–983. <https://ieeexplore.ieee.org/document/8968092/>, doi:10.1109/IROS40897.2019.8968092.
- Czyżżak, P., Jaskiewicz, A., 1998. Pareto simulated annealing—a metaheuristic technique for multiple-objective combinatorial optimization. *Journal of Multi-Criteria Decision Analysis* 7, 34–47. [https://onlinelibrary.wiley.com/doi/10.1002/\(SICI\)1099-1360\(199801\)7:1<34::AID-MCDA161>3.0.CO;2-6](https://onlinelibrary.wiley.com/doi/10.1002/(SICI)1099-1360(199801)7:1<34::AID-MCDA161>3.0.CO;2-6), doi:10.1002/(SICI)1099-1360(199801)7:1<34::AID-MCDA161>3.0.CO;2-6.
- Duan, Y., Schulman, J., Chen, X., Bartlett, P.L., Sutskever, I., Abbeel, P., 2016. RL²: Fast Reinforcement Learning via Slow Reinforcement Learning. <https://arxiv.org/abs/1611.02779>, doi:10.48550/ARXIV.1611.02779. version Number: 2.
- Felten, F., Alegre, L.N., Nowé, A., Bazzan, A.L.C., Talbi, E.G., Danoy, G., Silva, B.C.d., 2023a. A toolkit for reliable benchmarking and research in multi-objective reinforcement learning, in: *Proceedings of the 37th conference on neural information processing systems (NeurIPS 2023)*.
- Felten, F., Talbi, E.G., Danoy, G., 2023b. Multi-Objective Reinforcement Learning Based on Decomposition: A Taxonomy and Framework <https://arxiv.org/abs/2311.12495>, doi:10.48550/ARXIV.2311.12495. version Number: 2.
- Finn, C., Abbeel, P., Levine, S., 2017. Model-Agnostic Meta-Learning for Fast Adaptation of Deep Networks. <https://arxiv.org/abs/1703.03400>, doi:10.48550/ARXIV.1703.03400. version Number: 3.
- Hayes, C.F., Rădulescu, R., Bargiacchi, E., Källström, J., Macfarlane, M., Reymond, M., Verstraeten, T., Zintgraf, L.M., Dazeley, R., Heintz, F., Howley, E., Irissappane, A.A., Mannion, P., Nowé, A., Ramos, G., Restelli, M., Vamplew, P., Roijers, D.M., 2022. A practical guide to multi-objective reinforcement learning and planning. *Autonomous Agents and Multi-Agent Systems* 36, 26. <https://link.springer.com/10.1007/s10458-022-09552-y>, doi:10.1007/s10458-022-09552-y.

- Liang, E., Liaw, R., Moritz, P., Nishihara, R., Fox, R., Goldberg, K., Gonzalez, J.E., Jordan, M.I., Stoica, I., 2017. RLlib: Abstractions for Distributed Reinforcement Learning. <https://arxiv.org/abs/1712.09381>, doi:10.48550/ARXIV.1712.09381. version Number: 4.
- Liu, F.Y., Qian, C., 2021. Prediction Guided Meta-Learning for Multi-Objective Reinforcement Learning, in: 2021 IEEE Congress on Evolutionary Computation (CEC), IEEE, Kraków, Poland. pp. 2171–2178. <https://ieeexplore.ieee.org/document/9504972/>, doi:10.1109/CEC45853.2021.9504972.
- Lu, J., Mannion, P., Mason, K., 2024. A Meta-Learning Approach for Multi-Objective Reinforcement Learning in Sustainable Home Environments. <https://arxiv.org/abs/2407.11489>, doi:10.48550/ARXIV.2407.11489. version Number: 1.
- Nichol, A., Achiam, J., Schulman, J., 2018. On First-Order Meta-Learning Algorithms. <https://arxiv.org/abs/1803.02999>, doi:10.48550/ARXIV.1803.02999. version Number: 3.
- Rachman, R., Tingey, J., Allmendinger, R., Shukla, P., Pan, W., 2025. Multi-objective Sequential Decision Making for Holistic Supply Chain Optimization, in: Singh, H., Ray, T., Knowles, J., Li, X., Branke, J., Wang, B., Oyama, A. (Eds.), Evolutionary Multi-Criterion Optimization. Springer Nature Singapore, Singapore. volume 15512, pp. 259–274. https://link.springer.com/10.1007/978-981-96-3506-1_18, doi:10.1007/978-981-96-3506-1_18. series Title: Lecture Notes in Computer Science.
- Rachman, R., Tingey, J., Allmendinger, R., Shukla, P., Pan, W., 2026. Reinforcement learning for multi-objective multi-echelon supply chain optimisation. *European Journal of Operational Research* , S0377221726001177<https://linkinghub.elsevier.com/retrieve/pii/S0377221726001177>, doi:10.1016/j.ejor.2026.02.002.
- Reymond, M., Bargiacchi, E., Nowé, A., 2022. Pareto Conditioned Networks, in: Pareto Conditioned Networks.
- Schmidhuber, J., 1987. Evolutionary principles in self-referential learning. Ph.D. thesis.
- Schulman, J., Wolski, F., Dhariwal, P., Radford, A., Klimov, O., 2017. Proximal Policy Optimization Algorithms <https://arxiv.org/abs/1707.06347>, doi:10.48550/ARXIV.1707.06347. version Number: 2.
- Shar, I.E., Wang, H., Gupta, C., 2023. Multi-Objective Reinforcement Learning for Sustainable Supply Chain Optimization, in: 2023 IEEE 19th International Conference on Automation Science and Engineering (CASE), IEEE, Auckland, New Zealand. pp. 1–7. <https://ieeexplore.ieee.org/document/10260354/>, doi:10.1109/CASE56687.2023.10260354.
- Sutton, R.S., Barto, A.G., 2015. Reinforcement Learning: An Introduction. 1st ed., The MIT Press, Massachusetts.

- Thrun, S., Pratt, L., 1998. Learning to Learn: Introduction and Overview, in: Thrun, S., Pratt, L. (Eds.), Learning to Learn. Springer US, Boston, MA, pp. 3–17. http://link.springer.com/10.1007/978-1-4615-5529-2_1, doi:10.1007/978-1-4615-5529-2_1.
- Van Moffaert, K., Drugan, M.M., Nowe, A., 2013. Scalarized multi-objective reinforcement learning: Novel design techniques, in: 2013 IEEE Symposium on Adaptive Dynamic Programming and Reinforcement Learning (ADPRL), IEEE, Singapore, Singapore. pp. 191–199. <http://ieeexplore.ieee.org/document/6615007/>, doi:10.1109/ADPRL.2013.6615007.
- Wang, Q., Zhang, C., Hu, B., 2024. Dynamic programming with meta-reinforcement learning: a novel approach for multi-objective optimization. Complex & Intelligent Systems 10, 5743–5758. <https://link.springer.com/10.1007/s40747-024-01469-1>, doi:10.1007/s40747-024-01469-1.
- Xu, J., Tian, Y., Ma, P., Rus, D., Sueda, S., Matusik, W., 2020. Prediction-guided multi-objective reinforcement learning for continuous robot control, in: III, H.D., Singh, A. (Eds.), Proceedings of the 37th international conference on machine learning, PMLR. pp. 10607–10616. <https://proceedings.mlr.press/v119/xu20h.html>.
- Yang, R., Sun, X., Narasimhan, K., 2019. A Generalized Algorithm for Multi-Objective Reinforcement Learning and Policy Adaptation <https://arxiv.org/abs/1908.08342>, doi:10.48550/ARXIV.1908.08342. version Number: 2.
- Zhang, Z., Wu, Z., Zhang, H., Wang, J., 2023. Meta-Learning-Based Deep Reinforcement Learning for Multiobjective Optimization Problems. IEEE Transactions on Neural Networks and Learning Systems 34, 7978–7991. <https://ieeexplore.ieee.org/document/9714721/>, doi:10.1109/TNNLS.2022.3148435.
- Zhao, T., Lou, J., 2025. Research on the application of deep learning in low-carbon supply chain management. International Journal of Low-Carbon Technologies 20, 209–216. <https://academic.oup.com/ijlct/article/doi/10.1093/ijlct/ctae290/7990584>, doi:10.1093/ijlct/ctae290.
- Zitzler, E., Thiele, L., 1998. Multiobjective optimization using evolutionary algorithms — A comparative case study, in: Goos, G., Hartmanis, J., Van Leeuwen, J., Eiben, A.E., Bäck, T., Schoenauer, M., Schwefel, H.P. (Eds.), Parallel Problem Solving from Nature — PPSN V. Springer Berlin Heidelberg, Berlin, Heidelberg. volume 1498, pp. 292–301. <http://link.springer.com/10.1007/BFb0056872>, doi:10.1007/BFb0056872. series Title: Lecture Notes in Computer Science.

SUPPLEMENTARY MATERIAL OF MIRACL: A Diverse Meta-Reinforcement Learning for Multi-Objective Multi-Echelon Combinatorial Supply Chain Optimisation

A Notations

Table 1: The nodes i , j , and k symbolise the SC network facilities, with period t as the daily interval. The variables ς , ψ , and τ signify inventory, production, and transport activities.

Notations	Definition
q_{ij}^τ	Transport quantity at period t , from node i to j
q_{tk}^ψ	Manufacturing quantity at period t , at manufacturer k
$Prof$	Total profit of all periods
E	Total emission of all periods
F	Total SL inequality measure of all periods
SL_y	SL at node y of all periods
Rev_t	Revenue at period t
PC_t	Production cost at period t
TC_t	Transport cost at period t
IC_t	Inventory cost at period t
L	Transport lead time
I_{tj}	Inventory unit at period t , node j
c_j^ς	Inventory cost per unit at node j
e_j^ς	Emission per unit resulted from inventory at node j
c_k^ψ	Manufacturing cost per unit at node k
v_k^ψ	Yield ratio from manufacturing process at node k
e_k^ψ	Emission per unit resulted from the manufacturing process at node k
c_{ij}^τ	Transport cost per unit from node i to j
e_{ij}^τ	Emission per unit resulted from product transport from node i to j
\mathbf{Q}_{tj}	The outstanding order at node j
CE_t	The accumulated emission at period t
AF_t	The average service level inequality in period t
d_{tz}	Demand at period t , market z
Cap	Transport capacity

B Problem Definition: MOMDP-Based Formulation

The supply chain (SC) problem simulated in this paper adopts the SC optimisation problem based on the multi-objective Markov decision process (MOMDP) as referred to in the main text. We extended the problem to simpler and more complex SC networks for our experiments. N^s, N^m, N^d , and N^r represent sets of suppliers, manufacturers, distributors, and retailers respectively. For completeness purposes, we restate the formulation here.

B.1 State Transition Functions

State transition describes the shift of functions from the state at period $(t - 1)$ to period t , as defined by Equations (1) to (4):

$$I_{tj} = I_{(t-1)j} + \sum_{i \in (N^s \cup N^m \cup N^d)} q_{(t-L)ij}^\tau - \sum_{k \in (N^d \cup N^r \cup N^z)} q_{tjk}^\tau, \quad \forall j \in (N^m \cup N^d \cup N^r), \text{ where } i < j < k \quad (1)$$

$$\mathbf{Q}_{tj} = \{q_{(t-L+1)ij}^\tau, \dots, q_{tij}^\tau \mid \forall j \in (N^m \cup N^d \cup N^r), i \in (N^s \cup N^m \cup N^d), \text{ such that } i < j\} \quad (2)$$

$$CE_t = CE_{(t-1)} + E_t \quad (3)$$

$$AF_t = \frac{AF_{t-1} \cdot (t-1) + F_t}{t}. \quad (4)$$

B.2 State Space (S)

At each timestep, the agents' observation of the simulation environment is described by the state. The state at period t is defined as follows:

$$\mathbf{S}_t = \{I_{(t-1)j}, \mathbf{Q}_{(t-1)j}, CE_{t-1}, AF_{t-1} \mid 0 \leq I_{(t-1)j}, \forall j \in (N^m \cup N^d \cup N^r)\}. \quad (5)$$

B.3 Action Space (A)

In our SC environment, the actions at period t are given by:

$$\mathbf{A}_t = \{q_{tij}^\tau, q_{tik}^\psi \mid 0 \leq q_{tij}^\tau \leq Cap, \quad 0 \leq q_{tik}^\psi, \forall i \in (N^s \cup N^m \cup N^d), j \in (N^m \cup N^d \cup N^r), k \in N^m, \text{ where } i < j\}. \quad (6)$$

B.4 Rewards (R)

The problem has three goals: maximise profit while minimising greenhouse gas (GHG) emissions and service level (SL) inequality. Multi-objective reinforcement learning (MORL) agents maximise cumulative rewards with negative values for GHG emissions and SL inequality, resulting in the reward vector $\mathbf{R}_t = \{Prof_t, -E_t, -F_t\}$. Each objective is computed as follows:

$$Prof_t = \left(\sum_{i \in N^d} \sum_{j \in N^r} q_{(t-L)ij}^\tau \cdot price \right) - \left(\sum_{k \in N^m} \frac{q_{tik}^\psi \cdot c_k^\psi}{v_k^\psi} \right) - \left(\sum_{i \in (N^s \cup N^m \cup N^d)} \sum_{j \in (N^m \cup N^d \cup N^r)} q_{tij}^\tau \cdot c_{ij}^\tau \cdot L \right) - \left(\sum_{j \in (N^m \cup N^d \cup N^r)} I_{tj} \cdot c_j^\xi \right), \quad \text{where } i < j, \quad (7)$$

$$E_t = \sum_{j \in (N^m \cup N^d \cup N^r)} (I_{tj} \cdot e_j^\xi) + \sum_{k \in N^m} (q_{tk}^\psi \cdot e_k^\psi) + \sum_{i \in (N^s \cup N^m \cup N^d)} \sum_{j \in (N^m \cup N^d \cup N^r)} (q_{ij}^\tau \cdot e_{ij}^\tau \cdot L), \quad (8)$$

where $i < j$,

$$F_t = \frac{1}{2} \sum_{y \in N^r} \sum_{\substack{y' \in N^r \\ y' \neq y}} |SL_{ty} - SL_{ty'}|. \quad (9)$$

While this model reference operates on deterministic cases, our SC environments involve uncertainties arising from lead time, cost, emissions, and market demand.

C Fine-Tuning Algorithm

The pseudocode of the fine-tuning mechanism is given in Algorithm 1.

Algorithm 1 Fine-tuning Phase of MIRACL

Require: Trained meta-policy π_θ , unseen task $\mathcal{T}_{\text{new}} \sim p(\mathcal{T})$, number of solutions K , fine-tuning steps T , PSA fine-tuning steps T_{add}

- 1: **Initialise:** archive $PF \leftarrow \emptyset$
 - 2: Generate K normalised weights $\{\mathbf{w}_1, \dots, \mathbf{w}_K\}$ on the simplex
 - 3: **for** $k = 1$ to K **do**
 - 4: Form subproblem \mathcal{T}_k using $(\mathcal{T}_{\text{new}}, \mathbf{w}_k)$
 - 5: Rollout \mathcal{D}_k using π_θ in \mathcal{T}_k for T steps
 - 6: Compute adapted parameters θ'_k from \mathcal{D}_k
 - 7: Evaluate reward \mathbf{r}_k in \mathcal{T}_k using $\pi_{\theta'_k}$
 - 8: **end for**
 - 9: Update $\mathbf{w}, PF \leftarrow \text{DiversityMechanism}(\mathcal{T}_{\text{new}}, \mathbf{w}, \mathbf{r}, PF)$
 - 10: **for** $k = 1$ to K **do**
 - 11: Form updated subproblem \mathcal{T}_k using current \mathbf{w}_k
 - 12: Rollout additional D_k in \mathcal{T}_k and compute additional updates on θ'_k for T_{add} steps
 - 13: Evaluate vector reward \mathbf{r}_k in \mathcal{T}_k using $\pi_{\theta'_k}$
 - 14: **end for**
 - 15: **Return:** Fine-tuned policies $\{\pi_{\theta'_k}\}_{k=1}^K$, weights $\{\mathbf{w}_k\}_{k=1}^K$, updated PF
-

D Simulated Environment

Our experiment employs three SC environments: simple, moderate, and complex networks. SC networks are node collections linked by edges, with parameters set at nodes and edges. Each network is 'fully connected', linking all nodes across consecutive layers. Material supply from suppliers is treated as unlimited. Market demand is unstable: markets one and two fluctuate as normal distributions ($\mu = 150, \sigma = 60$ and $\mu = 100, \sigma = 40$) and markets three, four, and five as Poisson distributions ($\lambda = 200, 100, 150$). Seasonal demand shifts through sinusoidal-modulated distributions. Simple SC serves markets 1 and 2, moderate SC covers markets 1-3, and complex SC involves all markets.

For simple SC markets, a fixed mean price of 20 is applied, while moderate and complex SC markets encounter variable mean prices: [20, 21, 20.5] and [100, 101, 105, 103, 104]. Unfulfilled demand is regarded as demand loss. This problem is structured within the MOMDP framework with a finite time horizon $T = 100$ and a lead time range of $L = \{1, 3\}$ days. The transportation capacity (Cap) is set at 200, while the manufacturing capacity is not restricted.

To simulate uncertainties originating mainly from demand, cost, price structure, and lead time, we randomise the parameters during environment generations. For example, in addition to the fluctuation of demand along the period horizon, we also introduce randomised mean and standard deviation values within a range of $\{90\%, 110\%\}$ of set values. A similar range is also applied to the costs and prices, subject to the task arrangement scenarios applied. During fine-tuning, new unseen tasks are given in the Table 2 to 7.

Table 2: **Simple SC.** Node parameter values that correspond to the facilities in Simple SC environment.

Node	I_{0j}	c_j^s	e_j^s	c_k^ψ	v_k^ψ	e_k^ψ
3	380	0.1100	0.0002	2.0000	1.0000	5.0126
4	350	0.1300	0.0002	2.2000	1.0000	4.5754
5	400	0.1200	0.0002	NA	NA	NA
6	80	0.1500	0.0002	NA	NA	NA

Table 3: Transport parameter values that correspond to product delivery.

From Node	To Node	c_{ij}^r	e_{ij}^r
1	2	0.2200	0.1258
	3	0.6900	0.3947
2	4	1.0550	0.6035
	5	0.4300	0.2460
3	4	0.4850	0.2774
	5	0.7500	0.4290

Table 4: **Moderate SC.** Node parameter values that correspond to the facilities in Moderate SC environment.

Node	I_{0j}	c_j^s	e_j^s	c_k^ψ	v_k^ψ	e_k^ψ
3	380	0.1100	0.0002	2.0000	1.0000	5.0126
4	350	0.1300	0.0002	2.2000	1.0000	4.5754
5	400	0.1200	0.0002	2.3000	1.0000	5.4491
6	80	0.1500	0.0002	NA	NA	NA
7	110	0.2000	0.0002	NA	NA	NA
8	100	0.2500	0.0002	NA	NA	NA
9	80	0.3000	0.0002	NA	NA	NA
10	120	0.2000	0.0002	NA	NA	NA

Table 5: Transport parameter values that correspond to product delivery.

From Node	To Node	c_{ij}^{τ}	e_{ij}^{τ}
1	3	0.2200	0.1258
	4	0.6900	0.3947
	5	0.5650	0.3232
2	3	1.0550	0.6035
	4	0.6500	0.3718
	5	0.6300	0.3604
3	6	0.0750	0.0429
	7	0.4300	0.2460
4	6	0.6300	0.3604
	7	0.2300	0.1316
5	6	0.4950	0.2831
	7	0.0750	0.0429
6	8	1.0950	0.6263
	9	0.6250	0.3575
	10	0.9500	0.5434
7	8	1.6400	0.9381
	9	1.1600	0.6635
	10	0.5800	0.3318

Table 6: **Complex SC.** Node parameter values that correspond to the facilities in Complex SC environment.

Node	I_{0j}	c_j^{ζ}	e_j^{ζ}	c_k^{ψ}	v_k^{ψ}	e_k^{ψ}
4	155	0.2300	0.0002	2.0000	1.0000	5.0126
5	267	0.3500	0.0002	2.2000	1.0000	4.5754
6	342	0.2200	0.0002	2.1000	1.0000	5.4491
7	211	0.1100	0.0002	2.0000	1.0000	6.1232
8	162	0.2900	0.0002	2.3000	1.0000	5.5157
9	195	0.3700	0.0002	NA	NA	NA
10	333	0.1100	0.0002	NA	NA	NA
11	96	0.3600	0.0002	NA	NA	NA
12	285	0.3300	0.0002	NA	NA	NA
13	68	0.2600	0.0002	NA	NA	NA
14	379	0.3000	0.0002	NA	NA	NA
15	344	0.1700	0.0002	NA	NA	NA
16	66	0.2900	0.0002	NA	NA	NA
17	356	0.2700	0.0002	NA	NA	NA
18	382	0.2300	0.0002	NA	NA	NA
19	362	0.3700	0.0002	NA	NA	NA

Table 7: Transport parameter values that correspond to product delivery.

From Node	To Node	c_{ij}^T	e_{ij}^T
1	4	0.5350	0.3060
	5	0.2650	0.1516
	6	1.8450	1.0553
	7	1.6000	0.9152
	8	1.4400	0.8237
2	4	0.3600	0.2059
	5	0.2950	0.1687
	6	1.2350	0.7064
	7	0.6250	0.3575
	8	1.8550	1.0611
3	4	0.6000	0.3432
	5	0.1750	0.1001
	6	0.7450	0.4261
	7	1.3300	0.7608
	8	0.1700	0.0972
4	9	1.9900	1.1383
	10	0.3400	0.1945
	11	0.8100	0.4633
5	9	1.5150	0.8666
	10	0.6600	0.3775
	11	0.6450	0.3689
6	9	1.6950	0.9695
	10	1.5800	0.9038
	11	0.8150	0.4662

From Node	To Node	c_{ij}^T	e_{ij}^T
7	9	1.6150	0.9238
	10	1.2600	0.7207
	11	0.6750	0.3861
8	9	1.0300	0.5892
	10	1.0900	0.6235
	11	1.6300	0.9324
9	12	1.9650	1.1240
	13	1.9250	1.1011
	14	1.6200	0.9266
10	8	1.4900	0.8523
	9	1.9600	1.1211
	10	0.6350	0.3632
11	8	1.8700	1.0696
	9	0.2000	0.1144
	10	1.8550	1.0611
12	15	1.9450	1.1125
	16	0.9650	0.5520
	17	1.9050	1.0897
	18	0.9000	0.5148
	19	0.6900	0.3947
13	15	0.8050	0.4605
	16	1.0650	0.6092
	17	1.8400	1.0525
	18	0.8300	0.4748
	19	1.8850	1.0782
14	15	1.6600	0.9495
	16	1.5100	0.8637
	17	0.5900	0.3375
	18	0.4000	0.2288
	19	1.3950	0.7979

E Detailed Algorithm Settings

This section provides the detailed hyperparameters used in our experiment.

E.1 Meta-training settings

Table 8 and 9 show the algorithm settings we used for MIRACL and Meta-MORL during our experiments.

Table 8: Hyperparameters for MAML-based meta-training.

Hyperparameter	Value
Inner-loop learning rate α	0.003
Outer-loop learning rate β	0.001
PPO steps per meta-update	10
Adaptation steps	4–8
Network architecture	[64, 64]
Discount factor γ	0.99
GAE weight	1.0
VF loss coefficient	0.5
Clipping parameter	0.3
KL target	0.01
KL coefficient	0.001
Batch size	32
Fragment length	32
Rollout workers	4
Evaluation interval	100

E.2 Fine-tuning settings

Table 9: PPO hyperparameters used in fine-tuning.

Hyperparameter	Value
Learning rate	3×10^{-4}
Steps per update	2048
Minibatch size	64
Epochs per update	10
Discount factor γ	0.99
GAE weight λ	0.95
Clipping range	0.2
Entropy coefficient	0
VF loss coefficient	0.5
Max gradient norm	0.5
Episode length	100
Total timesteps	5×10^5
Activation	Tanh

E.3 MORL with decomposition (MORL/D) setup

Table 10 shows the setup used for the MORL/D algorithm as one of the baselines.

Table 10: Hyperparameters of MORL/D Algorithm with MOSAC Policy

Hyperparameters	Values
MORL/D	
Discount factor	0.995
Population size	6
Exchange every	5×10^4
Total time steps	5×10^5
Neighbourhood size	1
Update passes	10
Initial weight dist.	uniform
MOSAC	
Buffer size	10^6
Discount factor	0.99
Target smoothing coef.	0.005
Batch size	128
Steps before learning	10^3
Hidden neurons	[256; 256]
Actor LR	3×10^{-4}
Critic LR	10^{-3}
Actor training freq.	2
Target training freq.	1
Activation function	ReLU

E.4 Non-dominated sorting genetic algorithm II (NSGA-II) setup

Table 11 shows the setup used in NSGA-II as one of the baselines.

Table 11: Hyperparameters of NSGA-II to solve the SC problem across three network complexities: simple, moderate, and complex.

Hyperparameters	Values
Population size	300
Offspring number	30
Cross-over operator	binary (SBX)
Cross-over probability	90%
Cross-over η	15
Mutation method	polynomial
Mutation η	20

F Performance Details

F.1 Traditional Method Comparison: Extended Analysis

Figure 1 presents a comparison of sparsity and EUM between the proposed MIRACL, Meta-MORL approach, and traditional RL methods.

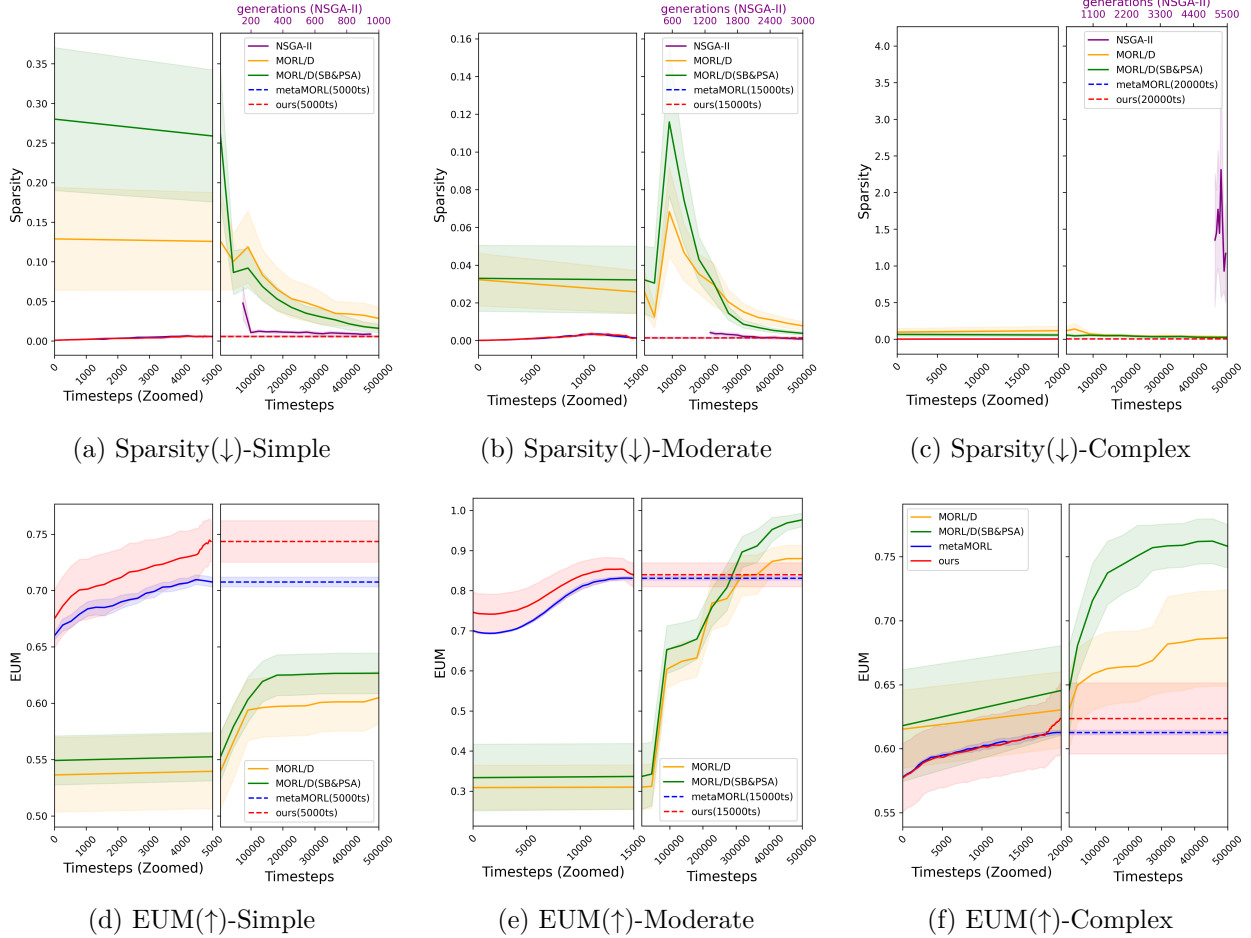


Figure 1: Sparsity and EUM of NSGA-II, MORL/D, MORL/D with SB and PSA, Meta-MORL, and our proposed algorithms. The left parts are zoomed in on the early timesteps with meta-learning, while the right parts show MORL/D timesteps and NSGA-II generations. The EUM reveal that meta-learning methods outperform MORL/D in simpler problems but increasingly struggle with more complex ones. Normalised sparsity consistently shows the lowest values for meta-learning-based methods across all complexities.

F.2 Ablation Study

Table 12: Ablation study for MIRACL on simple SC (mean over 10 runs), where *, **, *** denote statistically significant differences: $p < 0.05$, $p < 0.01$, and $p < 0.001$, respectively. The Kruskal–Wallis followed with Dunn’s post hoc (Bonferroni-corrected) is used for data sets > 2 , and the Wilcoxon test for data sets = 2. Bold text represents the baseline value of each parameter.

Setting	Hypervolume	Sparsity	EUM
<i>Number of subproblems K</i>			
$K = 3$	0.3832***	0.0088	0.7156
$K = 5$	0.4003*	0.0064	0.7146
$K = 10$	0.4387	0.0076	0.7141
<i>PSA steps S</i>			
$S = 3$	0.4371	0.0060	0.7055**
$S = 5$	0.4487	0.0070	0.7108
$S = 10$	0.4592	0.0063	0.7155
<i>PSA rate δ</i>			
$\delta = 0.03$	0.4550	0.0060	0.7156
$\delta = 0.05$	0.4512	0.0071	0.7150
$\delta = \mathbf{0.10}$	0.4564	0.0071	0.7122
<i>Scalarisation methods</i>			
Linear	0.4600	0.0057	0.7436
Tchebycheff	0.4630	0.0081***	0.7148***

Table 12 suggests three practical configuration insights for MIRACL on simple SC. First, too few subproblems degrades the learned frontier, so increasing K matters more than marginal tuning elsewhere. Second, reducing PSA depth harms EUM more than hypervolume, indicating PSA is key for steering the archive toward solutions preferred under the evaluation weight distribution, not merely enlarging the dominated region. Third, Tchebycheff yields a more dispersed frontier but lower utility, whereas linear scalarisation gives the strongest preference-weighted performance. Overall, MIRACL is relatively insensitive to δ , while K and PSA depth S are the main levers for coverage and preference-aligned performances.

F.3 PF Approximate

Figure 2 shows the resulting solutions for each method from different points of view to complement the main text.

F.4 Operational Behaviour

Figure 3 displays the daily output levels from all manufacturing plants as determined by the solutions obtained from the three methods. We evaluate the operational behaviour of the solutions to understand their practical implications, focusing on manufacturing stability, inventory fluctuations, and unmet demand. A representative solution from the PF approximation set of each method is selected using the approximate proportion of objective values. Our proposed approach consistently

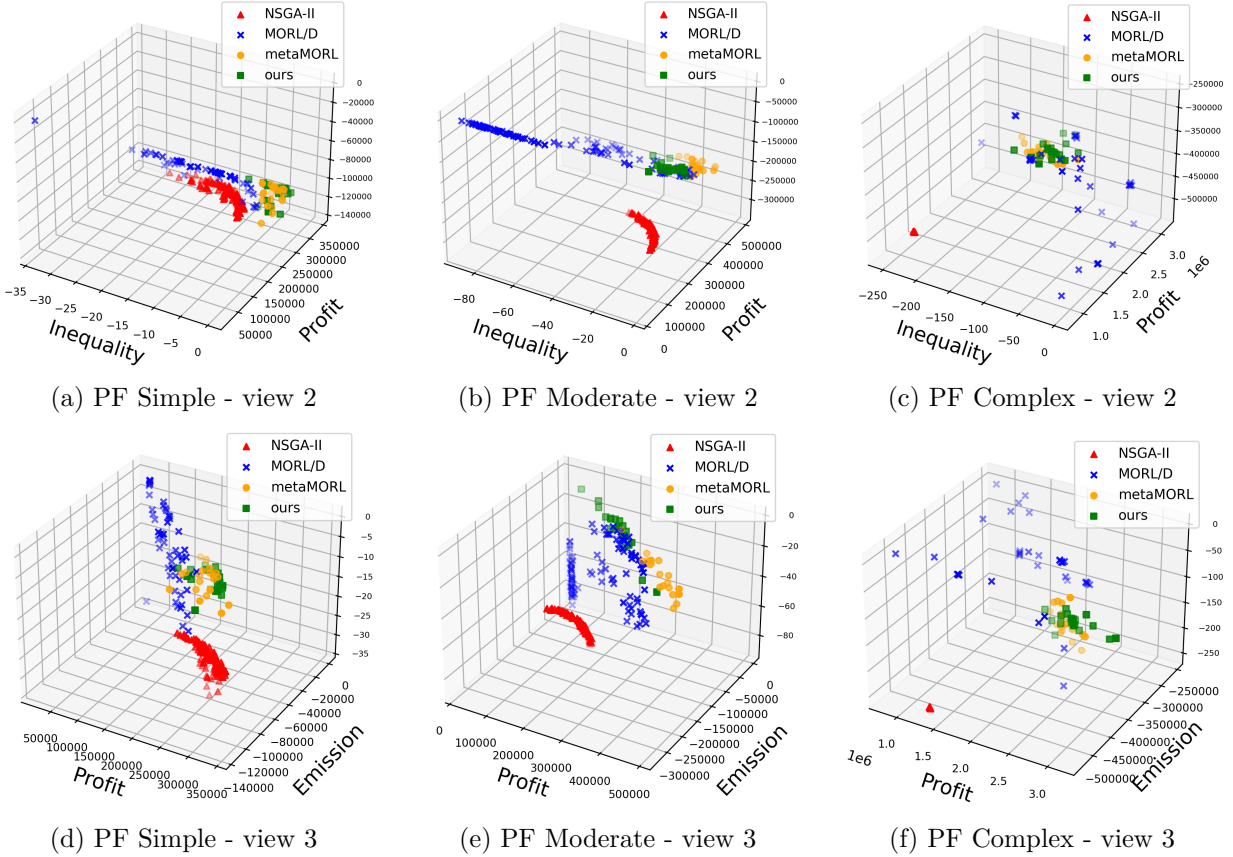


Figure 2: PF approximation sets between algorithms in all problem complexities. In general, meta-learning-based algorithms reside in a narrower solution space. The solutions consistently spread in the range of moderate to high values of profit and GHG emissions, while low to moderate values of SL inequality in all problem complexities.

yields stable and evenly distributed manufacturing quantities, avoiding the erratic production patterns observed in MORL/D and NSGA-II. This stability reflects the generalisation property of meta-learning, which prioritises consistent behaviour over reactive adjustments.

Figure 4 depicts the comparison of daily inventory levels across the three supply chain problems when using MIRACL compared to traditional methods. In terms of inventory management, our proposed method maintains leaner and stable inventory levels with low variance, compared to MORL/D and NSGA-II. In complex problems, it buffers selectively at key facilities to manage uncertainty while avoiding widespread overstocking. Regarding unmet demand, our proposed method achieves a comparable demand loss in all problems without excessive inventory. These behaviours highlight the practicality of meta-learning-based approaches for achieving stable and balanced operations in SC environments.

F.5 Demand Loss

Figure 5 shows the comparison of the loss of demand in all corresponding markets and in all methods.

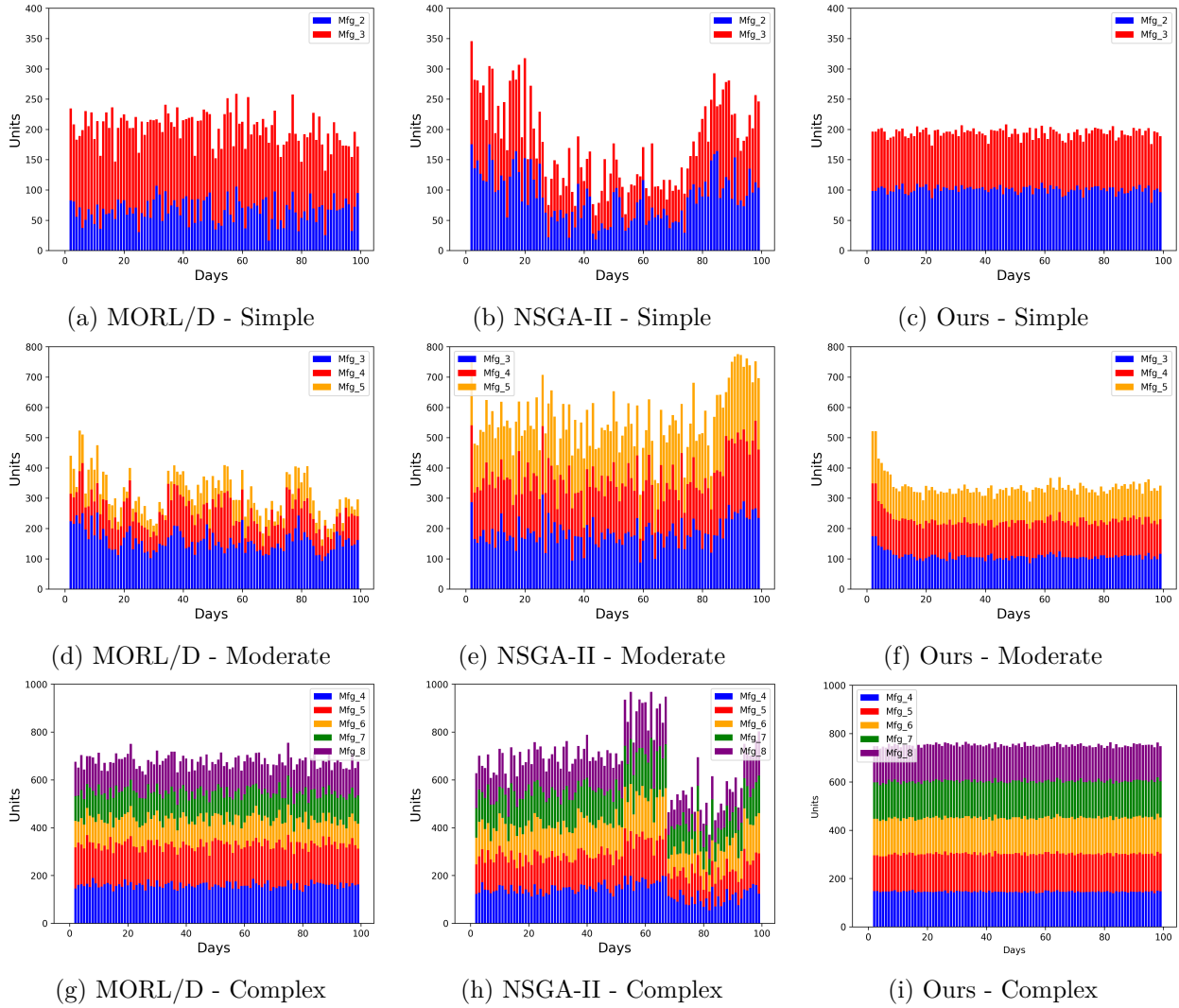


Figure 3: Manufacturing quantities of three algorithms. Our proposed method (3c,3f,3i) exhibits the most stable daily production quantities and evenly distributed production amounts across facilities compared to MORL/D and NSGA-II.

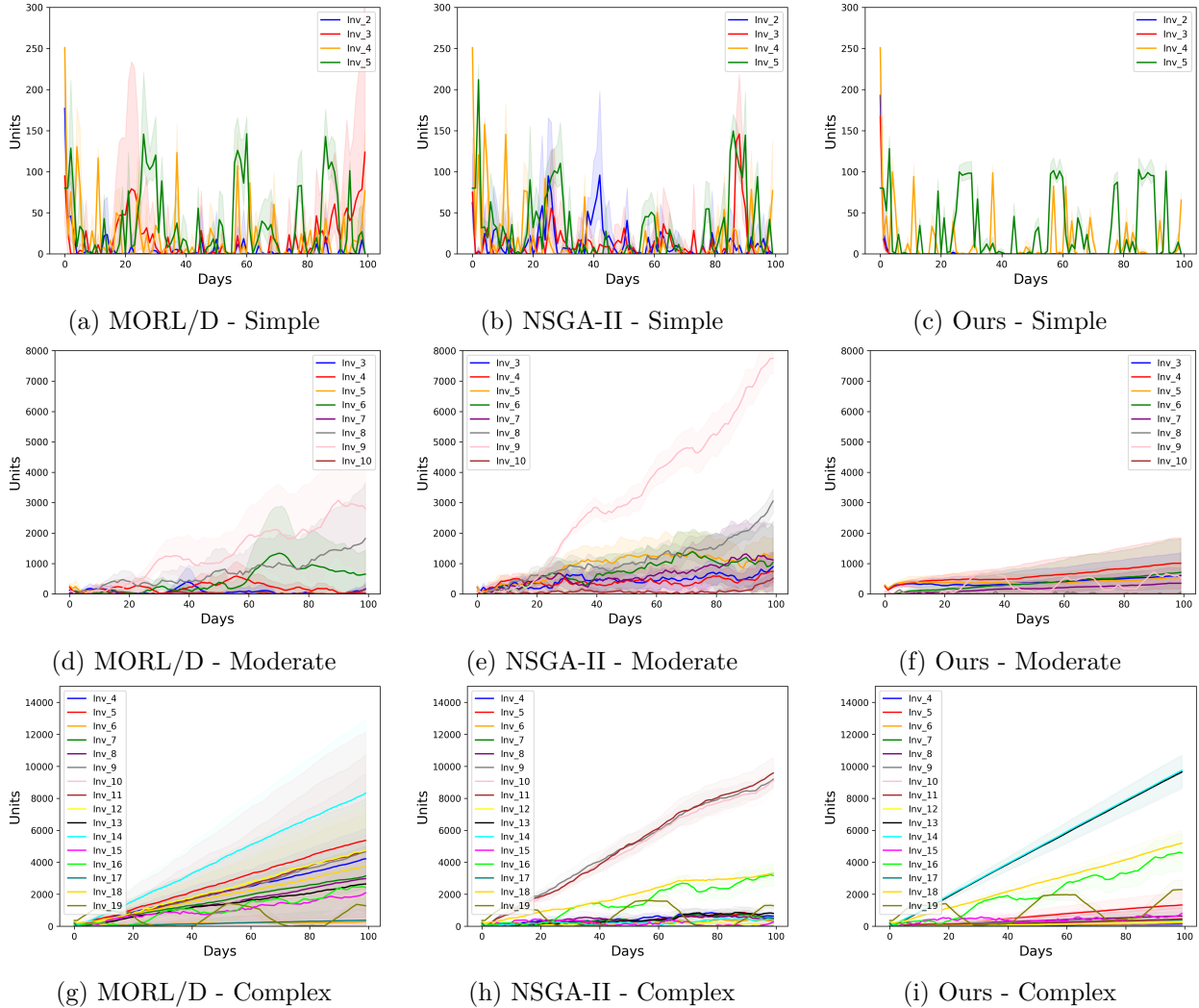


Figure 4: The inventory levels yielded from the three algorithms in various complexities. Our proposed method (4c,4f,4i) exhibits relatively lean and stable inventory levels daily compared to conventional RL. The average inventory levels tend to increase with the problem complexities for all algorithms.

